Since January 2020 Elsevier has created a COVID-19 resource centre with free information in English and Mandarin on the novel coronavirus COVID-19. The COVID-19 resource centre is hosted on Elsevier Connect, the company's public news and information website.

Informatics in Medicine Unlocked 22 (2021) 100506

Contents lists available at ScienceDirect

Informatics in Medicine Unlocked

journal homepage: http://www.elsevier.com/locate/imu

FCOD: Fast COVID-19 Detector based on deep learning techniques

Amir Hossein Panahi, Alireza Rafiei, Alireza Rezaee *

Faculty of New Sciences and Technologies, University of Tehran, Tehran, Iran

ARTICLE INFO

Keywords:
Deep learning
COVID-19 detection
Medical applications
Image processing
Radiology images
Chest X-ray images

ABSTRACT

The sudden COVID-19 pandemic has caused a serious global concern due to infections and mortality rates. It is a hazardous disease that has recently become the biggest crisis in the modern era. Due to the limitation of test kits and the need for screening and rapid diagnosis of patients, it is essential to perform a self-operating detection model as a fast recognition system to detect COVID-19 infection and prevent the spread among the people. In this paper, we propose a novel technique called Fast COVID-19 Detector (FCOD) to have a fast detection of COVID-19 using X-ray images. The FCOD is a deep learning model based on the Inception architecture that uses 17 depthwise separable convolution layers to detect COVID-19. Depthwise separable convolution layers decrease the computation costs, time, and they can have a reducing role in the number of parameters compared to the standard convolution layers. To evaluate FCOD, we used covid-chestxray-dataset, which contains 940 publicly available typical chest X-ray images. Our results show that FCOD can provide accuracy, F1-score, and AUC of 96%, 96%, and 0.95%, respectively in classifying COVID-19 during 0.014 s for each case. The proposed model can be employed as a supportive decision-making system to assist radiologists in clinics and hospitals to screen patients immediately.

1. Introduction

The coronavirus illness (COVID-19) is a universal pandemic that was found in December 2019 by a Chinese doctor in Wuhan, China [1]. Below the electron microscopes, the shape of these viruses is similar to the solar corona; accordingly, the researchists called them CoV [2]. The coronavirus family can cause serious infections and diseases like Middle East Respiratory Syndrome (MERS-CoV) and Severe Acute Respiratory Syndrome (SARS-CoV). On Feb 2020, the World Health Organization (WHO) called the pandemic COVID-19 because of the type of virus [3]. It has led to more than forty million infections and over one million deaths globally (up to Oct 20, 2020).

The sputum's assay via polymerase chain reaction (RT-PCR) is one of Coronaviruses recognition's principal standards, but RT-PCR is a time-consuming process for the patients to identify COVID-19 [4]. Accordingly, medical imaging modalities, like Computed Tomography (CT) and Chest X-ray (CXR), can be a significant task in checking positive COVID-19 infections, specifically about pregnant women on the way and children [5,6]. Volumetric CT thorax images have been studied in some previous researches for recognizing COVID-19 [5,7]. The main limitation of using the CT method is high cost and time-consuming [8]. In contrast, X-ray systems are accessible in most clinics and hospitals, which are used to generate 2-dimensional visualization images of the patient's rib cage.

Usually, the CXR manner is a premier option, which helps the radiologists to identify the chest pathology. According to the COVID-19 condition, the CXR manner is being utilized to detect COVID-19 [5,9]. Hence, the focus of this study is entirely on the use of X-ray imaging to potentially detect COVID-19 patients.

Fig. 1 shows a COVID-19 patient case with pneumonia chest X-ray images for a week is given. The patient, when using CT, may get more amount of radiation compared to the X-ray. Hence, in some cases, it is suggested to utilize X-ray imagery [8,10]. Computer-Aided Diagnosis (CAD) systems have been extended to overcome this limitation and help physicians to identify suspected diseases of vital organs in X-ray images automatically [11,12]. These systems, which are chiefly supported by the fast and advanced of computer technology (like CPU, GPU, and, TPU) are used to operate the medical vision computing algorithms, containing image enhancement, classification, segmentation, and tumor detection tasks [13–15]. In several medical fields, Artificial intelligence (AI) methods like a deep neural network and machine learning turn to the core of the superior CAD applications. In recent years, deep learning methods have encouraged the results to perform radiological tasks by automated examining multi-modal medical images [16–18]. Deep

* Corresponding author.
E-mail address: arrezaee@ut.ac.ir (A. Rezaee).

https://doi.org/10.1016/j.imu.2020.100506
Received 21 October 2020; Received in revised form 15 December 2020; Accepted 16 December 2020
Available online 24 December 2020

learning techniques are one of the robust neural network structures. In an intuitional way been used in several practical applications in several practical usages, such as image segmentation and classification [19]. The use of machine learning techniques in the medical area for automated analysis has gained a new reputation by developing an assistive tool for clinicians [20–24]. Deep learning technique, which is one of the modern research fields of AI, provides the development of end-to-end methods to attain promised outcomes applying input information, in the absence of handy feature exploitation [25,26]. However, deep learning methods have been strongly used in various challenges like skin disease classification [27,28], arrhythmia identification [29–31], brain damages classification [32], breast cancer recognition [33,34], fundus image segmentation [35], pneumonia detection from chest X-ray images [36], and segmentation of the lung [37,38].

The rapid development of COVID-19 outbreaks necessitates the development of automated detection algorithms based on AI methods. Due to the limited number of radiologists in different areas, it is challenging to provide specialist clinicians for each hospital. Also, accurate, fast, and simple AI algorithms can address this issue and present practical assistance for the patients. Radiologist's wide experience in this area plays a key role; in radiology, the AI equipment may help to gain a precise diagnosis [39]. Besides, AI programs may be valuable in reducing the disadvantages such as an inadequate quantity of possible RT-PCR test kits and test costs. In this paper, we proposed a fast and accurate deep learning model for the detection of COVID-19 from X-ray images. Notwithstanding overlapping features, the proposed intelligent network can classify COVID-19 and normal cases into different classes. Early detection in the case of COVID-19 plays an essential role in the handling of the disease. Currently, the detection is made for patients by a set of laboratory experiments. These experiments are a time-consuming process and need commercial kits. Also, researchers affirm that merging laboratory outcomes with clinical image characteristics can be used in the early detection of COVID-19 [40–42]. Radiologic data, such as images collected from COVID-19 cases, include valuable data for diagnostic and treatment. Some analyses have found differences in chest X-ray and CT images since the onset of COVID-19 symptoms [43]. Hence, alternative methods of detection are essential in the case of COVID-19.

The Inception network is known as one of the Deep Convolutional Neural Network (DCNN) models with high capacity and high performance in the classification task. The primary Inception model was one of the most popular learning architectures for image processing tasks [44]. The proposed model in this research is based on the Inception structure. However, our innovation is that the middle layers change fundamentally, which is a new robust classification model. [1]

Accordingly, this study will present a new robust framework of deep learning classifiers as a high-level assistive implement to help the radiologists. It can automatically detect COVID-19 in X-ray images in clinics and hospitals. The overall contributions of this paper are reviewed in the following:

- Designing a new framework based on deep learning assists of COVID-19 detection.
- Analyzing the suggested classifier architecture to classify COVID-19 virus via using chest X-ray images to achieve a lower cost process and prediction time.
- Reporting the results of the proposed DCNN classifier model.
- The proposed framework supports researchers in developing high-level artificial intelligence methods for CAD devices to prevent the spread of the COVID-19 virus.

The rest of this paper is organized as follows: Section 2 gives a review of related works. System architecture, which contains the proposed model, is presented in section 3. We analyze the results of the suggested algorithm in section 4. The conclusion and discussion are given in the last section.

2. Related works

Many types of researches focus on COVID-19 diagnosis. In most studies, deep neural network methods are applied to chest X-ray models to recognize contagious and accurate results.

A DCNN model based on pre-trained transfer architectures (ResNet50 [45], InceptionV3 [44], and Inception-ResNetV2 [46]) that can predict the coronavirus infection from chest X-ray images, is proposed in Ref. [47]. The presented CNN based model showed excellent prediction performance and accuracy from a small sample of X-ray images classified into two classes, COVID-19 and normal cases. Moreover, to dominate the inadequate information and training time, a transfer learning manner is used by the ImageNet dataset [48]. The outcomes confirmed the superiority accuracy in pairs of the training and testing grade of the ResNet50 model.

Abbas et al. proposed a new CNN model based on class decomposition and transfer learning to get better performance of the X-ray image classification on pre-trained models [49]. The presented structure is called DeTraC and includes three stages. In the first stage, local feature extraction is performed by using ImageNet pre-trained CNN. In the second stage, a stochastic gradient descent (SGD) optimization approach is utilized for training. Finally, the class combination layer is adjusted for the image's ultimate classification by employing error-correction

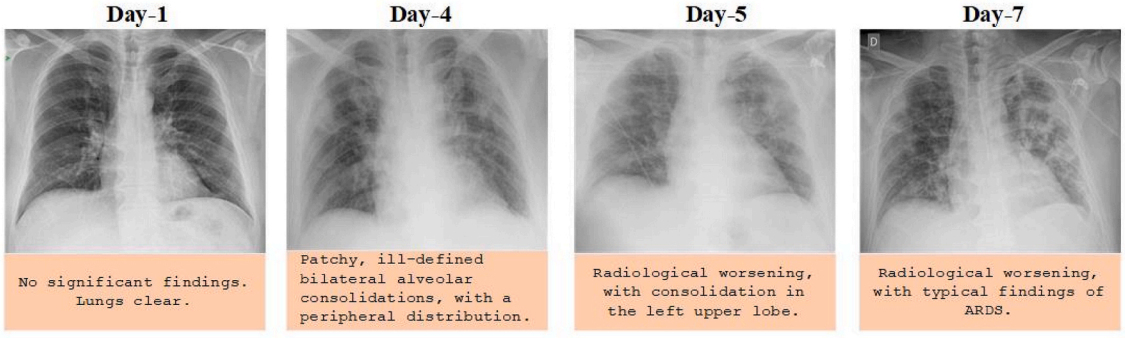

Fig. 1. Chest X-ray images of a 50-year-old COVID-19 patient case over a week.

criteria related to a softmax layer. The ResNet18 [45] pre-trained ImageNet architecture is applied, and the results show an accuracy of 95.12% on chest X-ray images.

Wand et al. introduced a DCNN called COVID-Net, which can detect

[1] Edgar Lorente, COVID-19 pneumonia - evolution over a week, https://radiopaedia.org.

COVID-19 patients from CXR images [50]. This architecture design includes two parts: a human-machine collaborative design approach and a machine-driven design exploration part. A lightweight residual projection-expansion-projection-extension (PEPX) design pattern is used in this architecture. Also, an explain ability-driven examination is executed for decision validation. The model results presented high sensitivity and precision of 87.1% and 96.4%, respectively, for the COVID-19 cases.

Hemdan et al. proposed a structure to classifying COVID-19 disease from chest X-ray images containing seven image classifiers named COVIDX-Net with high performance and accuracy of 90% for the DenseNet201 and VGG19 classifiers [51]. Hassanien et al. presented a classification method to detect COVID-19 in lung X-ray images that utilize multi-level thresholding and a SVM [52]. Their algorithm was tested on 40 contrast-enhanced lung X-ray images. Their classification method gained a sensitivity of 95.76%, a specificity of 99.7%, and an accuracy of 97.48%.

Zhang et al. proposed a novel deep anomaly detection method formed on CXR images for the screening of COVID-19 [53]. This proposed network includes some parts. The high-level features of images were extracted and then used as the input. The classification part is utilized for the image classification and is composed of a hidden convolutional layer of 100-neurons. The scalar anomaly scores are generated in the anomaly detection part (COVID-19 cases). The suggested architecture attained the false positive rate. The results illustrated a specificity and sensitivity of 70.65% and 96.00%, respectively.

3. Materials and methods

3.1. Data set

In this study, we have used a publicly available dataset that exists in the GitHub repository,[2] which has been collected by Ref. [54]. This dataset includes X-ray images of patients infected with COVID-19, SARS, Pneumocystis, and other types of pneumonia. We just analyzed the 940 COVID-19 and Non-COVID-19 X-ray cases and divided them into two parts, 80% for the training and 20% for testing the model. In Fig. 2 some examples of the dataset are shown. The statistical characteristics (mean, minimum, and maximum) of the dataset's images are tabulated in Table 1.

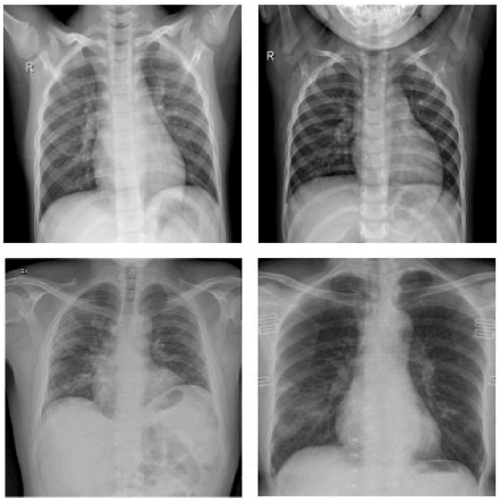

Fig. 2. Some examples from dataset. The first row are normal cases, and the second are COVID-19 cases.

[2] https://github.com/ieee8023/covid-chestxray-dataset.

Table 1
The statistical mean, minimum, and maximum of width and height of the dataset's classes.

Type	Images count	Min Width	Max width	Min height	Max height
Covid	435	137	4300	156	4300
Non-Covid	505	224	224	224	224
Mean	–	180.5	2262	190	2262

3.2. Data augmentation

Data augmentation is a popular operation applied in deep learning, which enlargement the amount of available training/testing data [55]. In this work, due to the lack of the required number of available samples, data augmentation techniques were accomplished by ImageDataGenerator in the training task. The transformations function applied random rotation in the range of 20°, width and height shift operations in the range of 0.2 pixels, zooming operation in the range of 0.8 and 1.2, and horizontal flips. ImageDataGenerator has finally produced 3760 images for the training phase of the proposed model. Data augmentation improves and enhances the network's ability to learn. Data augmentation is an effective method to prohibit network overfitting by increasing the number of training samples [56].

3.3. Depthwise separable convolutions layers

CNN's can automatically extract features, and cause the network to accomplish processing with high performance. Due to the high number of parameters, CNN has some restrictions on the computation cost, and the network overfitting. These limitations of CNN can be improved by using depthwise separable convolution that has been used in a neural network as early as 2014 [57].

Depthwise separable convolutions decrease computation cost, time, and the number of parameters. They use convolutional neural processes while improving the representational performance. Depthwise separable convolution layers are decreasing the number of parameters needed to operate at a given step, and they are more successful in image classification algorithms in achieving superior models.

Standard convolution executes the channel-wise and spatial-wise computation in one step. However, our proposed network is based on depthwise separable convolution, a standard 3×3 convolution layer divided into a 3×3 depthwise convolution and a 1×1 pointwise convolution. Depthwise separable convolution layer divided the computation into two steps: depthwise convolution and pointwise convolution. Depthwise convolution uses a convolutional filter per input channel, and pointwise convolution is utilized to mix the resulting output channels. Fig. 3 shows the comparison of standard convolution and depthwise separable convolution.

Suppose that K is a standard convolutional filter which size is $W \times W \times M \times N$, and F is an input feature map which size is $D_f \times D_f \times M$. By applying a standard convolution on an input feature map produces an output feature map O which size is $D_f \times D_f \times N$,

$$O_{k,l,n} = \sum_{i,j,m} K_{i,j,m,n} \cdot F_{k+i-1,l+j-1,m} \quad (1)$$

In depthwise separable convolution, this computation is divided into two levels. The first level uses a 3×3 depthwise convolution $\widehat{K}$ to input channel,

$$\widehat{O}_{k,l,m} = \sum_{i,j} \widehat{K}_{i,j,m,n} \cdot F_{k+i-1,l+j-1,m} \quad (2)$$

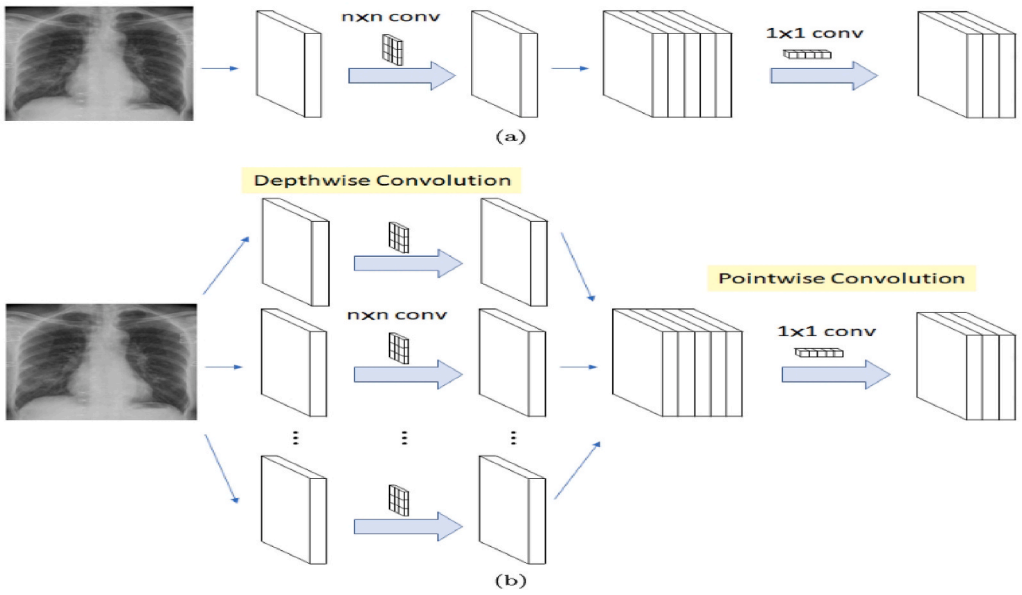

Fig. 3. (a) Standard CNN. (b) Depthwise Separable CNN. In depthwise separable convolution, standard convolutional layers divided into two different levels. Depthwise convolution executes convolution in a single depth slice, while pointwise Convolution merges the information over the entire depth.

The second level exerts 1×1 pointwise convolution $\overline{K}$, in order to merge the total output,

$$O_{k,l,n} = \sum_{m} \overline{K}_{m,n} \cdot \widehat{O}_{k-1,l-1,m} \tag{3}$$

Pointwise convolution and depthwise convolution have distinct tasks in producing new features: the first one is used for obtaining channel-wise correlations, while the second one is used for obtaining spatial correlations.

3.4. Activation function

Rectified Linear Unit (ReLU) is a non-linear activation function that is utilized in neural networks models, and is defined as:

$$f(x) = max(0, x) \tag{4}$$

where x is an input parameter. As stated in Eq (4), the maximum value between zero and function input is the ReLU output. When the input value is negative the output is equivalent to zero, and when the input is positive, the outcome is x. Accordingly, the Eq (4) readdress as follows:

$$f(x) = \begin{cases} 0, if\ x < 0 \\ x, if \geq 0 \end{cases} \tag{5}$$

In our proposed model, ReLU is used after each depthwise separable convolution layer. Relu is not a vanishing gradient, more computationally efficient, and learn several times faster [26].

3.5. Proposed model

In this section, we present the Fast COVID-19 Detector (FCOD) model as a deep learning model for automatic classification of COVID-19 in 2D X-ray images. FCOD has used depthwise separable convolution layers, which is shown in Fig. 4.

In the proposed model, we have been using fewer layers and filters in contrast to the basic architectures. Also, we have applied depthwise separable convolution layers instead of convolutional layers.

The model consists of three parts. In the first part, the chest X-ray images were used for the input layer of the model. These images pass over four depthwise separable convolution layers, and then the max-pooling layer follows each of the depthwise separable convolution layers. The middle part merged with 12 depthwise separable convolution layers. Both of the first and middle parts are followed by batch normalization.

Also, batch normalization enables significant gradients, and the results appear in faster convergence [58]. The dropout layer is utilized after 16 separable convolution layers with a dropout ratio of 0.2 [59]. This network ends with Global Average Pooling, a layer of depthwise separable convolution, two fully-connected (FC) layers, and a softmax activation function.

3.6. Model training

By updating the weights of the network, the loss function, which is a categorical cross-entropy can optimize the algorithm. Categorical cross-entropy is utilized for multi-class classification task to predict the probabilities over the N number of classes.

The RMSprop optimization algorithm is used for training the model [60]. We have set 100 epochs, 16 batch sizes, and a learning rate of 0.001 for training our network.

3.7. Classification performance

For analyzing the performance of each model, different metrics have been used. As shown in Fig. 5, we have used a confusion matrix for analyzing the performances of the proposed network.

This matrix has four expected parameters as follows: TP, TN, FP, FN which refer to the true positive, true negative, false positive, and false negative samples of any class. Accuracy is generally utilized as a classification metric and represents how well a classification model can distinguish the classes in the test set. The accuracy is defined by:

$$Accuracy = \frac{TP + TN}{TP + FP + FN + TN} \tag{6}$$

As shown in Eq (6), the accuracy can be explained as the ratio of the predicted correct labels of the structure over the total number of labels.

Precision (Eq (7)) is defined as the ratio of predicted correct labels of the architecture over the whole number of actual labels.

$$Precision = \frac{TP}{TP + FP} \tag{7}$$

Recall (Eq (8)) is defined as the proportion of predicted correct labels

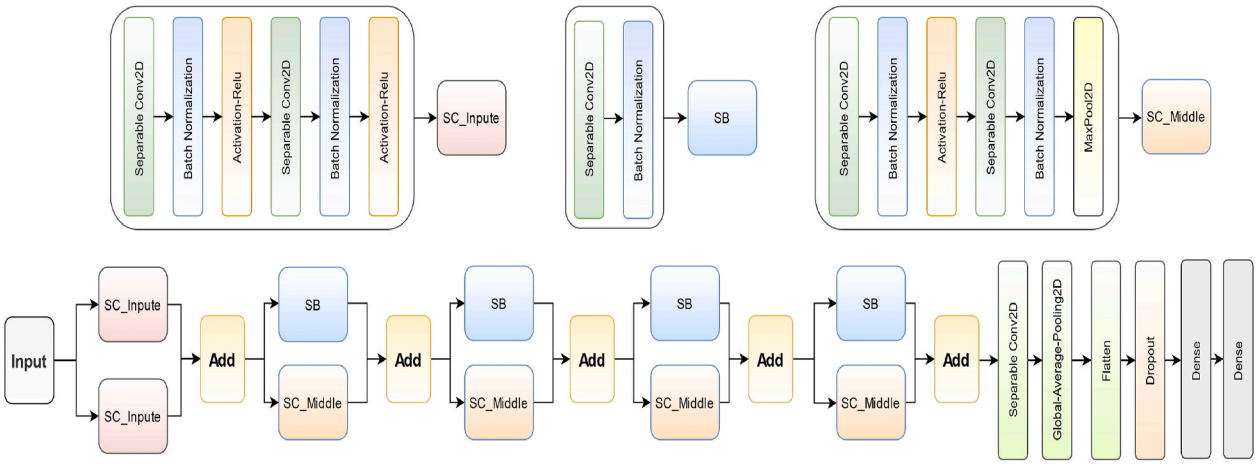

Fig. 4. Scheme of the proposed classifier architecture.

	Actually Positive (1)	Actually Negative (0)
Predicted Positive (1)	True Positives (TPs)	False Positives (FPs)
Predicted Negative (0)	False Negatives (FNs)	True Negatives (TNs)

Fig. 5. Confusion matrix.

of the model over the total number of predicted labels.

$$Recall = \frac{TP}{TP + FN} \tag{8}$$

Measuring the proportion of negatives which are recognized without error, is done by specificity (Eq (9)).

$$Specificity = \frac{TN}{FP + TN} \tag{9}$$

Also, F1 - score (Eq (10)) is referred to the harmonic average of the Precision and Recall.

$$F1 - score = 2\frac{(Precision \times Recall)}{(Precision + Recall)} \tag{10}$$

4. Experimental results

In this section, we show the performance of the proposed algorithm using various evaluation metrics.

The model is implemented in Python using Keras framework 2.2.4 with Tensorflow 1.14.0 as the backend, and the hardware configuration is based on free Google service.[3]

The Receiver Operating Characteristics (ROC) curve and the confusion matrix of the proposed model are shown in Fig. 6 (a) and 6(b), respectively.

The training and testing accuracy and loss curves of the proposed classification model are demonstrated in Fig. 7. As shown in this Figure, the loss value of the training and testing phases has decreased. On the other hand, the accuracy of the training and testing sets have increased. Accordingly, these issues indicate that the proposed architecture has appropriate efficiency.

The performance metrics of some popular deep learning classifier models are tabulated in Table 2.

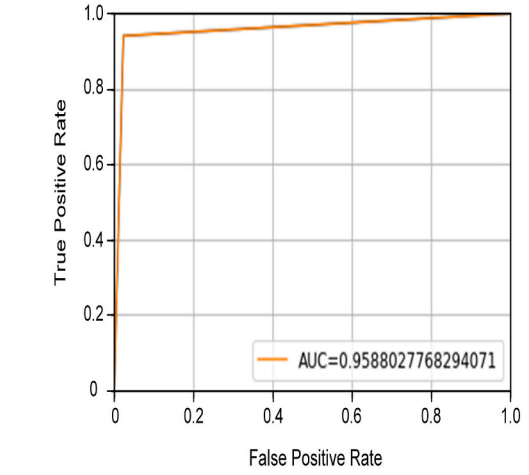

(a) Receiver Operating Charac-teristics (ROC) curve of the propsed model.

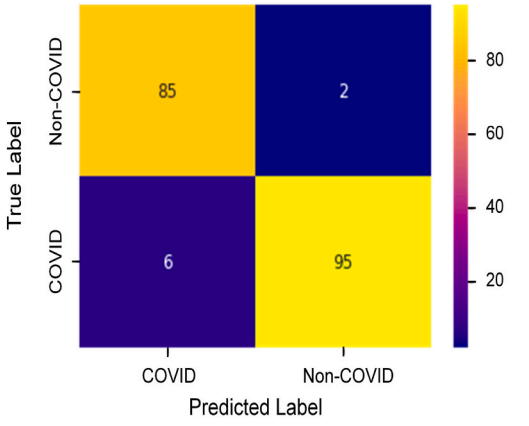

(b) Confusion matrix of the model.

Fig. 6. ROC curves and confusion matrix of the proposed deep learning model.

According to Table 2, the tested DCNN image classifier model's accuracy and computational times are compared with the other models. By using the GPU's robust abilities with a small X-ray image dataset, the proposed deep learning model's running time is low. Also, the overall

[3] https://colab.research.google.com.

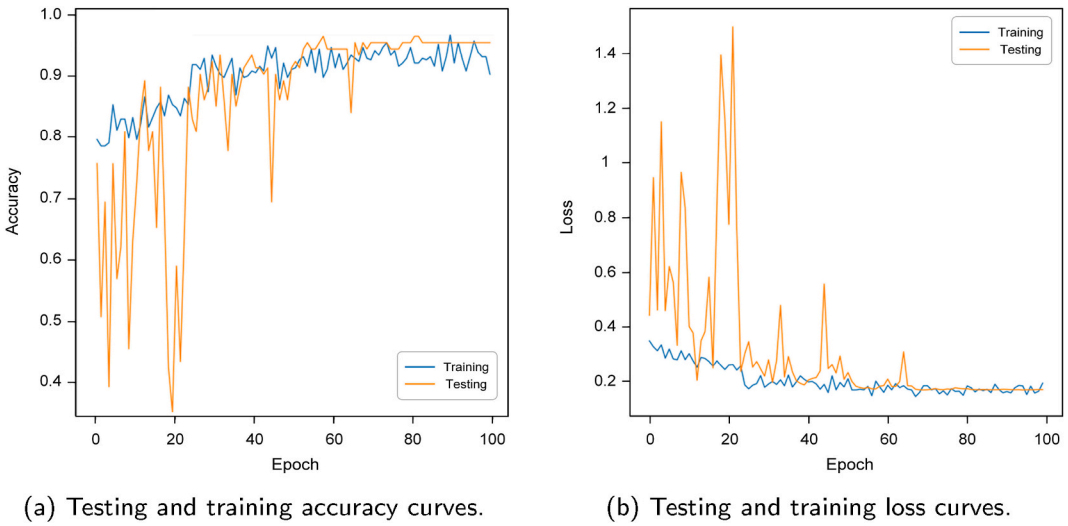

(a) Testing and training accuracy curves. (b) Testing and training loss curves.

Fig. 7. Accuracy and loss curves of the training and testing phases of the proposed deep learning model.

Table 2
Comparative classification performance of deep learning models.

Classifier	Sensitivity	Specificity	Precision	Accuracy	F1-Score	Training time(s)	Testing time(s)
COVID-Net [61]	0.90	0.80	–	0.85	0.22	–	–
COVID-CAPS [62]	0.90	0.95	–	0.95	–	–	–
Shashank [63]	098	0.91	0.96	0.96	0.97	–	–
VGG19 [51]	0.83	1.00	1.00	0.90	0.81	2641	4.0
CovidGAN [64]	0.95	0.94	0.90	0.94	0.92	–	–
ResNet50 [47]	–	100	100	0.98	0.98	–	–
DenseNet201 [51]	0.83	1.00	1.00	0.90	0.81	2122	6.00
ResNetV2 [51]	1.00	0.62	0.40	0.70	0.57	1086	2.00
InceptionV3 [51]	–	0.50	0.00	0.50	–	1121	2.00
Inception -ResNetV2 [51]	1.00	0.71	0.60	0.80	0.75	1988	6.00
Xception [51]	1.00	0.71	0.60	0.80	0.75	2035	3.00
MobileNetV2 [51]	1.00	0.55	0.20	0.60	0.33	389	1.00
Proposed Model	0.93	0.97	0.97	0.96	0.96	1800	0.014

accuracy is 96%, and the prediction time is 0.014 s, which is one of the best prediction times among the classifier models in this task. Eventually, this model can be used as an online/real-time framework with high accuracy and low prediction time.

The performance of FCOD for some randomly selected patients is shown in Fig. 8. FCOD can detect COVID-19 cases quickly with high accuracy.

5. Discussion and conclusion

Since the excessive infection rates and mortality of COVID-19 cases have been increasing, there is a need to use early, fast, and inexpensive

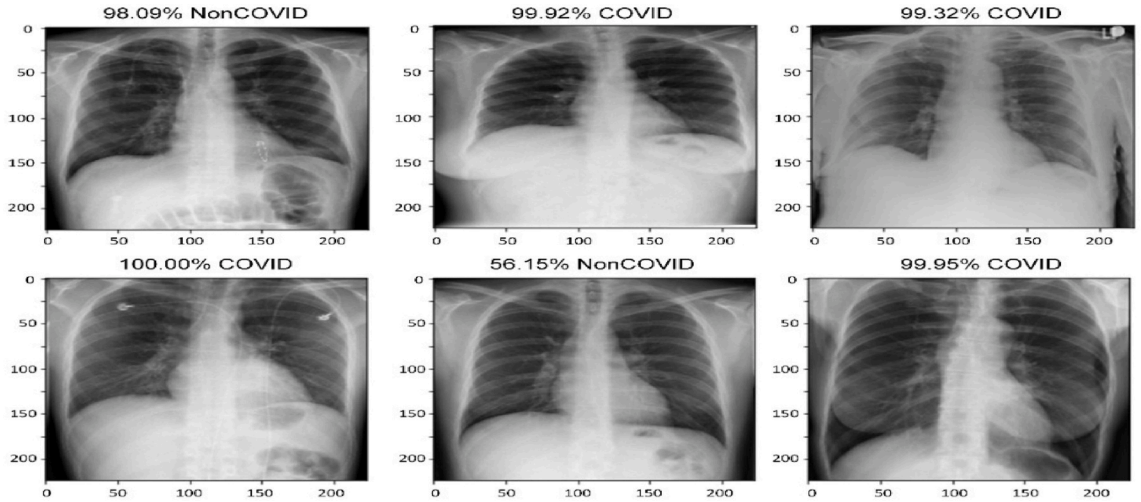

Fig. 8. Some examples from final output of the proposed model.

diagnostic methods. Unfortunately, there is still no specific drug or approved vaccine to treat COVID-19 infected patients, while fast diagnosis and screening of the disease are two basic and essential issues. Nowadays, most laboratories are equipped to detect the virus gaining the otorhinolaryngological methods.

The availability of testing devices and kits is the limitation of the COVID-19 tests. X-ray machines are more simply and quickly available. Hence, the use of chest X-ray images for analysis of the Coronavirus will be assistive. To address this issue, we proposed a novel architecture called FCOD, which has trained, tested, and validated on chest X-ray images for fast detection of COVID-19.

This network can be efficiently utilized to help doctors in the analysis of the X-ray images. The proposed algorithm's innovation has a lower prediction time than the other existing models with high performance. The network automatically recognizes the complicated patterns from X-ray images, which is comparable with skilled radiologists. Furthermore, we can improve our network's performance by adding more COVID cases of chest X-ray images in our training data.

The proposed classification method was tested and evaluated on covid-chestxray-dataset, which is a publicly available dataset. For comparison, we report the results with the other popular existing methods. The proposed network has illustrated essential improvements over the other methods, especially in prediction time. The proposed algorithm can perform detection of the COVID-19 in 0.014 s. The obtained accuracy and AUC for the proposed model are 96%, and 95%, respectively.

From what has been discussed above, it can be concluded that the proposed classification algorithm can be used as an accurate and fast method to detect COVID-19 using chest X-ray images. This model can be used as an online/real-time medical assistive implement in radiologic clinics and hospitals.

Declaration of competing interest

The authors declare that they have no known competing financial interests or personal relationships that could have appeared to influence the work reported in this paper.

Acknowledgment

None.

References

[1] Catharine I Paules, Marston Hilary D, Fauci Anthony S. Coronavirus infections—more than just the common cold. Jama 2020;323(8):707–8.
[2] Chen Yu, Liu Qianyun, Guo Deyin. Emerging coronaviruses: genome structure, replication, and pathogenesis. J Med Virol 2020;92(4):418–23.
[3] Sohrabi Catrin, Alsafi Zaid, O'Neill Niamh, Khan Mehdi, Ahmed Kerwan, Al-Jabir Ahmed, et al. World health organization declares global emergency: a review of the 2019 novel coronavirus (covid-19). Int J Surg 2020;76:71–6.
[4] Huang Peikai, Liu Tianzhu, Huang Lesheng, Liu Hailong, Lei Ming, Xu Wangdong, Hu Xiaolu, Chen Jun, Liu Bo. Use of chest ct in combination with negative rt-pcr assay for the 2019 novel coronavirus but high clinical suspicion. Radiology 2020;295(1):22–3.
[5] Ng Ming-Yen, Lee Elaine YP, Jin Yang, Yang Fangfang, Xia Li, Wang Hongxia, Mei-sze Lui Macy, Lo Christine Shing-Yen, Leung Barry, Khong Pek-Lan, et al. Imaging profile of the covid-19 infection: radiologic findings and literature review. Radiology: Cardiothorac. Imag. 2020;2(1):e200034.
[6] Liu Huanhuan, Liu Fang, Li Jinning, Zhang Tingting, Wang Dengbin, Lan Weishun. Clinical and ct imaging features of the covid-19 pneumonia: focus on pregnant women and children. J Infect 2020;80(5):7–13.
[7] Chung Michael, Adam Bernheim, Mei Xueyan, Zhang Ning, Huang Mingqian, Zeng Xianjun, Cui Jiufa, Xu Wenjian, Yang Yang, Fayad Zahi A, et al. Ct imaging features of 2019 novel coronavirus (2019-ncov). Radiology 2020;295(1):202–7.
[8] Lucia JM Kroft, van der Velden Levinia, Hernández Girón Irene, Roelofs Joost JH, de Roos Albert, Geleijns Jacob. Added value of ultra–low-dose computed tomography, dose equivalent to chest x-ray radiography, for diagnosing chest pathology. J Thorac Imag 2019;34(3):179.
[9] Chen Nanshan, Zhou Min, Dong Xuan, Qu Jieming, Gong Fengyun, Han Yang, Qiu Yang, Wang Jingli, Liu Ying, Yuan Wei, et al. Epidemiological and clinical characteristics of 99 cases of 2019 novel coronavirus pneumonia in wuhan, China: a descriptive study. Lancet 2020;395(10223):507–13.
[10] Esmail Karar Mohamed, Merk Denis R, Falk Volkmar, Oliver Burgert. A simple and accurate method for computer-aided transapical aortic valve replacement. Comput Med Imag Graph 2016;50:31–41.
[11] Merk Denis R, Esmail Karar Mohamed, Chalopin Claire, Holzhey David, Falk Volkmar, Mohr Friedrich W, Oliver Burgert. Image-guided transapical aortic valve implantation sensorless tracking of stenotic valve landmarks in live fluoroscopic images. Innovations 2011;6(4):231–6.
[12] Messerli Michael, Kluckert Thomas, Knitel Meinhard, Rengier Fabian, Warschkow René, Alkadhi Hatem, Leschka Sebastian, Wildermuth Simon, Bauer Ralf W. Computer-aided detection (cad) of solid pulmonary nodules in chest x-ray equivalent ultralow dose chest ct-first in-vivo results at dose levels of 0.13 msv. Eur J Radiol 2016;85(12):2217–24.
[13] Tian Xiangdong, Wang Jian, Du Dongfeng, Li Shuwen, Han Changxiao, Zhu Guangyu, Tan Yetong, Ma Sheng, Chen Handong, Lei Ming. Medical imaging and diagnosis of subpatellar vertebrae based on improved laplacian image enhancement algorithm. Comput Methods Progr Biomed 2020;187:105082.
[14] Tao He, Hu Junjie, Song Ying, Guo Jixiang, Zhang Yi. Multi-task learning for the segmentation of organs at risk with label dependence. Med Image Anal 2020;61:101666.
[15] Hannan Richard, Free Matthew, Arora Varun, Harle Robin, Paul Harvie. Accuracy of computer navigation in total knee arthroplasty: a prospective computed tomography-based study. Medical Engineering & Physics; 2020.
[16] Chen Liang, Bentley Paul, Mori Kensaku, Misawa Kazunari, Fujiwara Michitaka, Rueckert Daniel. Self-supervised learning for medical image analysis using image context restoration. Med Image Anal 2019;58:101539.
[17] Gao Fei, Yoon Hyunsoo, Wu Teresa, Chu Xianghua. A feature transfer enabled multi-task deep learning model on medical imaging. Expert Syst Appl 2020;143:112957.
[18] Kim Minjeong, Yan Chenggang, Yang Defu, Wang Qian, Ma Junbo, Wu Guorong. Deep learning in biomedical image analysis. In: Biomedical information technology. Elsevier; 2020. p. 239–63.
[19] Zhou Ding-Xuan. Theory of deep convolutional neural networks: Downsampling. Neural Network 2020;124:319–27.
[20] Litjens Geert, Kooi Thijs, Ehteshami Bejnordi Babak, Arindra Adiyoso Setio Arnaud, Ciompi Francesco, Ghafoorian Mohsen, Awm Van Der Laak Jeroen, Van Ginneken Bram, I Sánchez Clara. A survey on deep learning in medical image analysis. Med Image Anal 2017;42:60–88.
[21] Ker Justin, Wang Lipo, Rao Jai, Lim Tchoyoson. Deep learning applications in medical image analysis. Ieee Access 2017;6:9375–89.
[22] Shen Dinggang, Wu Guorong, Suk Heung-Il. Deep learning in medical image analysis. Annu Rev Biomed Eng 2017;19:221–48.
[23] Faust Oliver, Hagiwara Yuki, Hong Tan Jen, Lih Oh Shu, Acharya U Rajendra. Deep learning for healthcare applications based on physiological signals: a review. Comput Methods Progr Biomed 2018;161:1–13.
[24] Murat Fatma, Yildirim Ozal, Talo Muhammed, Baran Baloglu Ulas, Demir Yakup, Acharya U Rajendra. Application of deep learning techniques for heartbeats detection using ecg signals-analysis and review. Comput Biol Med 2020:103726.
[25] LeCun Yann, Bengio Yoshua, Hinton Geoffrey. Deep learning. Nature 2015;521(7553):436–44.
[26] Krizhevsky Alex, Sutskever Ilya, Hinton Geoffrey E. Imagenet classification with deep convolutional neural networks. Advances in neural information processing systems. 2012. p. 1097–105.
[27] Estava A, Kuprel B, Novoa RA, et al. Dermatologist level classification of skin cancer with deep neural networks [j]. Nature 2017;542:115.
[28] Codella Noel CF, Nguyen Q-B, Pankanti Sharath, Gutman David A, Helba Brian, Halpern Allan C, Smith John R. Deep learning ensembles for melanoma recognition in dermoscopy images. IBM J Res Dev 2017;61(4/5). 5–1.
[29] Yıldırım Özal, Pławiak Paweł, Tan Ru-San, Acharya U Rajendra. Arrhythmia detection using deep convolutional neural network with long duration ecg signals. Comput Biol Med 2018;102:411–20.
[30] Hannun Awni Y, Rajpurkar Pranav, Haghpanahi Masoumeh, Geoffrey H Tison, Bourn Codie, Turakhia Mintu P, Andrew Y Ng. Cardiologist-level arrhythmia detection and classification in ambulatory electrocardiograms using a deep neural network. Nat Med 2019;25(1):65.
[31] Acharya U Rajendra, Shu Lih Oh, Hagiwara Yuki, Tan Jen Hong, Adam Muhammad, Gertych Arkadiusz, San Tan Ru. A deep convolutional neural network model to classify heartbeats. Comput Biol Med 2017;89:389–96.
[32] Talo Muhammed, Yildirim Ozal, Baran Baloglu Ulas, Aydin Galip, Acharya U Rajendra. Convolutional neural networks for multi-class brain disease detection using mri images. Comput Med Imag Graph 2019;78:101673.
[33] Celik Yusuf, Talo Muhammed, Yildirim Ozal, Karabatak Murat, Acharya U Rajendra. Automated invasive ductal carcinoma detection based using deep transfer learning with whole-slide images. Pattern Recognition Letters; 2020.
[34] Cruz-Roa Angel, Basavanhally Ajay, González Fabio, Gilmore Hannah, Feldman Michael, Ganesan Shridar, Shih Natalie, Tomaszewski John, Madabhushi Anant. Automatic detection of invasive ductal carcinoma in whole slide images with convolutional neural networks. In: Medical imaging 2014: digital pathology. vol. 9041. International Society for Optics and Photonics; 2014, 904103.
[35] Tan Jen Hong, Fujita Hamido, Sivaprasad Sobha, Sulatha V Bhandary, Krishna Rao A, Kuang Chua Chua, Acharya U Rajendra. Automated segmentation of exudates, haemorrhages, microaneurysms using single convolutional neural network. Inf Sci 2017;420:66–76.

[36] Rajpurkar Pranav, Irvin Jeremy, Zhu Kaylie, Yang Brandon, Mehta Hershel, Duan Tony, Ding Daisy, Bagul Aarti, Curtis Langlotz, Shpanskaya Katie, et al. Chexnet: radiologist-level pneumonia detection on chest x-rays with deep learning. 2017. arXiv preprint arXiv:1711.05225.
[37] Gaál Gusztáv, Maga Balázs, Lukács András. Attention u-net based adversarial architectures for chest x-ray lung segmentation. 2020. arXiv preprint arXiv:2003.10304.
[38] Carvalho Souza Johnatan, Bandeira Diniz João Otávio, Ferreira Jonnison Lima, França da Silva Giovanni Lucca, Correa Silva Aristofanes, Cardoso de Paiva Anselmo. An automatic method for lung segmentation and reconstruction in chest x-ray using deep neural networks. Comput Methods Progr Biomed 2019;177:285–96.
[39] Caobelli Federico. Artificial intelligence in medical imaging: game over for radiologists? Eur J Radiol 2020;126:108940.
[40] Kong Weifang, Agarwal Prachi P. Chest imaging appearance of covid-19 infection. Radiology: Cardiothorac. Imag. 2020;2(1):e200028.
[41] Shi Heshui, Han Xiaoyu, Jiang Nanchuan, Cao Yukun, Alwalid Osamah, Gu Jin, et al. Radiological findings from 81 patients with covid-19 pneumonia in wuhan, China: a descriptive study. Lancet Infect Dis 2020;20(4):425–34.
[42] Li Yan, Xia Liming. Coronavirus disease 2019 (covid-19): role of chest ct in diagnosis and management. Am J Roentgenol 2020;214(6):1280–6.
[43] Chan Jasper Fuk-Woo, Yuan Shuofeng, Kok Kin-Hang, Wang To Kelvin Kai, Chu Hin, Jin Yang, Xing Fanfan, Liu Jieling, Yan Yip Cyril Chik, Poon Rosana Wing-Shan, et al. A familial cluster of pneumonia associated with the 2019 novel coronavirus indicating person-to-person transmission: a study of a family cluster. Lancet 2020;395(10223):514–23.
[44] Szegedy Christian, Vincent Vanhoucke, Sergey Ioffe, Shlens Jon, Wojna Zbigniew. Rethinking the inception architecture for computer vision. In: Proceedings of the IEEE conference on computer vision and pattern recognition; 2016. p. 2818–26.
[45] He Kaiming, Zhang Xiangyu, Ren Shaoqing, Sun Jian. Deep residual learning for image recognition. In: Proceedings of the IEEE conference on computer vision and pattern recognition; 2016. p. 770–8.
[46] Szegedy Christian, Sergey Ioffe, Vincent Vanhoucke, Alemi Alexander A. Inception-v4, inception-resnet and the impact of residual connections on learning. Thirty-first AAAI conference on artificial intelligence. 2017.
[47] Ali Narin, Kaya Ceren, Pamuk Ziynet. Automatic detection of coronavirus disease (covid-19) using x-ray images and deep convolutional neural networks. 2020. arXiv preprint arXiv:2003.10849.
[48] Jia Deng, Dong Wei, Socher Richard, Li Li-Jia, Li Kai, Fei-Fei Li. Imagenet: a large-scale hierarchical image database. In: 2009 IEEE conference on computer vision and pattern recognition. Ieee; 2009. p. 248–55.
[49] Abbas Asmaa, Abdelsamea Mohammed M, Gaber Mohamed Medhat. Classification of covid-19 in chest x-ray images using detrac deep convolutional neural network. 2020. arXiv preprint arXiv:2003.13815.
[50] Wang Linda, Wong Alexander. Covid-net: a tailored deep convolutional neural network design for detection of covid-19 cases from chest x-ray images. 2020. arXiv preprint arXiv:2003.09871.
[51] Din Hemdan Ezz El, Shouman Marwa A, Esmail Karar Mohamed. Covidx-net: a framework of deep learning classifiers to diagnose covid-19 in x-ray images. 2020. arXiv preprint arXiv:2003.11055.
[52] Ella Hassanien Aboul, Nabil Mahdy Lamia, Ali Ezzat Kadry, Haytham H Elmousalami, Hassan Aboul Ella. Automatic x-ray covid-19 lung image classification system based on multi-level thresholding and support vector machine. medRxiv; 2020.
[53] Zhang Jianpeng, Xie Yutong, Li Yi, Shen Chunhua, Xia Yong. Covid-19 screening on chest x-ray images using deep learning based anomaly detection. 2020. arXiv preprint arXiv:2003.12338.
[54] Cohen Joseph Paul, Morrison Paul, Lan Dao, Roth Karsten, Tim Q Duong, Ghassemi Marzyeh. Covid-19 image data collection: prospective predictions are the future. 2020. arXiv preprint arXiv:2006.11988.
[55] Mikołajczyk Agnieszka, Grochowski Michał. Data augmentation for improving deep learning in image classification problem. In: 2018 international interdisciplinary PhD workshop (IIPhDW). IEEE; 2018. p. 117–22.
[56] Perez Luis, Wang Jason. The effectiveness of data augmentation in image classification using deep learning. 2017. arXiv preprint arXiv:1712.04621.
[57] Laurent Sifre, Mallat Stéphane. Rigid-motion scattering for image classification. 2014. Ph. D. thesis.
[58] Sergey Ioffe, Szegedy Christian. Batch normalization: accelerating deep network training by reducing internal covariate shift. 2015. arXiv preprint arXiv:1502.03167.
[59] Srivastava Nitish, Hinton Geoffrey, Krizhevsky Alex, Sutskever Ilya, Salakhutdinov Ruslan. Dropout: a simple way to prevent neural networks from overfitting. J Mach Learn Res 2014;15(1):1929–58.
[60] Tieleman T, Hinton G. Divide the gradient by a running average of its recent magnitude. coursera: Neural Networks Machine Learn 2017. Technical Report, https://zh.coursera.org/learn/neuralnetworks/lecture/YQHki/rmsprop-divide-the-gradient-by-a-running-average-of-its-recent-magnitude.
[61] Tartaglione Enzo, Alberto Barbano Carlo, Berzovini Claudio, Calandri Marco, Grangetto Marco. Unveiling covid-19 from chest x-ray with deep learning: a hurdles race with small data. 2020. arXiv preprint arXiv:2004.05405.
[62] Afshar Parnian, Heidarian Shahin, Naderkhani Farnoosh, Oikonomou Anastasia, Plataniotis Konstantinos N, Mohammadi Arash. Covid-caps: a capsule network-based framework for identification of covid-19 cases from x-ray images. 2020. arXiv preprint arXiv:2004.02696.
[63] Vaid Shashank, Kalantar Reza, Bhandari Mohit. Deep learning covid-19 detection bias: accuracy through artificial intelligence. Int Orthop 2020;1.
[64] Abdul Waheed, Goyal Muskan, Gupta Deepak, Khanna Ashish, Al-Turjman Fadi, Rogerio Pinheiro Plácido. Covidgan: data augmentation using auxiliary classifier gan for improved covid-19 detection. IEEE Access 2020;8:91916–23.